NANOSYSTEMS: PHYSICS, CHEMISTRY, MATHEMATICS, 2014, 5 (4), P. 486–493

AB-INITIO STUDY OF Re AND Ru EFFECT ON STABILITY OF TCP NANOPARTICLES IN Ni-BASED SUPERALLOYS

N. I. Medvedeva, A. L. Ivanovskii

Institute of Solid State Chemistry UB RAS, Ekaterinburg, Russia

medvedeva@ihim.uran.ru

PACS 71.15.Mb 71.15.Nc 71.20.Be

Modern nickel-based superalloys contain high concentrations of rhenium that allows the improvement of their creep strength. The high levels of rhenium, however, results in the formation of topologically close-packed phases (TCP) which have a negative influence on its properties. The addition of ruthenium was found to reduce the precipitation of nano-sized TCP phases, but the reasons have not been established. In this paper, by using an ab-initio approach, we studied the effect of rhenium and ruthenium on the structural properties of Ni matrix as well as the TCP phases. We demonstrate that Cr, Mo and W are the most effective additions to provoke the formation of TCP phases, whereas ruthenium has a destabilizing effect.

Keywords: Ab initio calculations, rhenium effect, superalloys.

Received: 16 June 2014
Revised: 30 June 2014

1. Introduction

The high-temperature strength of Ni-based superalloys is achieved by adding refractory elements, such as molybdenum, tungsten, tantalum and rhenium [1-3]. Rhenium is the most effective solid solution strengthener and superalloys normally contain 3-6% of rhenium [1-4]. The addition of 6 %Re increases the creep and thermomechanical fatigue strength to 46% and 59% at 950°C. The third-generation of heat-resistant nickel alloys contain a high concentration of rhenium up to 9-12 % [5-7]. However, the higher level of rhenium results in the formation of topologically close-packed phases (TCP), which have a negative influence on the mechanical properties, since these particles serve as sites for crack initiation and cause embrittlement. The effects of solid-solution and precipitation strengthening are reduced due to the lower concentration of rhenium and other useful impurities in the γ and γ' matrices. The 4^{th}- and 5^{th}- generation superalloys contain lower Re concentrations up to 6% and addition of 3-6 % Ru which hinders formation of the undesirable TCP phases [7-12]. The mechanism by which ruthenium improves the microstructural stability is still under discussion [10-12] and thus, understanding the stability of TCP phases is crucial for the further development of superalloys.

The close-packed nanoparticles of different structural types (σ, μ, χ and A15 with space groups P42/mnm, R3m, Pnma and Pm3n, respectively) were observed in the rhenium-containing alloys [1-3]. It should be noted that the A15 structure is competitive with bcc and σ phases, and considered as a prototype of TCP phases [13-17]. The particles or thin films of A15 structure, known as β-W (Cr_3Si-type), were observed in the Cr, Mo and W alloys, as well as in the Fe–Cr, Ni–Cr and Co–Cr alloys. Nickel does not form ordered phases with rhenium or ruthenium, and the appearance of TCP particles is facilitated by the alloying elements,

which can change phase stability, diffusion of atoms and misfit of lattice parameters of γ and γ' phases. Group VI (W, Cr, Mo) impurities were observed to favor TCP formation and thus, the reduction of TCP phases may be achieved by their controlled concentration. Metastable particles of A15-type were predicted in the Cr–Re alloys from first-principles calculations [18,19]. Furthermore, *ab-initio* calculations [20] for Mo–Re and Mo–Ru demonstrated that the A15 phase has the greatest stability among other TCP binary phases (χ, σ, μ, C14, C36) within a small volume difference $\Delta V/V$ with bcc Mo.

The effect of impurities depends on their partitioning as well as their influence on the lattice parameters and elastic moduli of these phases (size and elastic misfit). The complexity of the eutectic ($\gamma + \gamma$') system makes it difficult to experimentally determine these changes under alloying. Empirical approaches [5] could not predict the mechanism of rhenium's effect on structural parameters and elastic moduli as well as the effect of interaction with other additives.

In this work, we present *ab-initio* study of the effects which rhenium and ruthenium have on the electronic structure, lattice parameters and elastic moduli of fcc Ni, as ascertained that rhenium and ruthenium is mainly distributed in the γ phase (the concentration of these impurities in the γ' phase is known to be more than an order of magnitude less). We also investigate the electronic structure and stability for the A15 elemental phases (Ni, Re, Ru, Cr, Mo, W) as well as binary M_3Re and M_3Ru phases (M=Ni, Cr, Mo, W). To elucidate the simultaneous presence of Ru and Re, we performed calculations for $M_3Re_{0.5}Ru_{0.5}$ (M=Ni, Cr, Mo, W). These simulations provide the reasons for the influence of d-impurities on the stability of topologically close-packed phases in Ni alloys.

2. Computational details

The calculations were performed by using the projector-augmented wave (PAW) method, as implemented in the Vienna *ab initio* simulation package (VASP) [21,22]. The generalized gradient approximation (GGA) in the Perdew–Burke–Ernzerhof (PBE) form [23] was employed for the exchange-correlation functional. Energy cutoff for plane-wave expansion of 400 eV and the k sampling with 8×8×8 k-points in the Brillouin zone were used for A15 structure, while elemental metals were calculated with 16×16×16 k-points. To study the effect of rhenium and ruthenium on the electronic structure and elastic properties of fcc Ni, we used 32-atom supercell, where one impurity atom (Re or Ru) was substituted for Ni atom that corresponds to the impurity concentration of 3 at.%. The A15 structure of M_3X consists of six equivalent M atoms in c site (0.25,0.25,0) which compose the pairs on each cube face and two X atoms in bcc positions with coordinates (0, 0, 0). To model A15 M_3X (X= Re,Ru) we followed to experimental findings [24] which established that transition metal atoms such as Cr occupy the twinned c positions and X atoms are in bcc a sites. The structural optimization was performed for the lattice parameters and atomic coordinates which were relaxed to their ground state by minimizing their Hellman–Feynman forces, using the conjugate gradient algorithm, until all interatomic forces were less than 0.1 eV/A°.

3. Results and discussion

3.1. Rhenium and ruthenium in fcc Ni

The calculated lattice parameters and elastic moduli for pure fcc Ni and Ni-3at.% Re (Ru) are listed in Table 1. First, the comparison of our results with experimental and theoretical data available for fcc Ni showed that these calculations provide reliable results. Furthermore, our calculations are in better agreement with the experimental data, especially

for elastic constants. Rhenium and ruthenium at 3at.% concentration increase the lattice parameter of fcc Ni by 0.34% and 0.30%, respectively, and the distances between the nearest Ni and Re (Ru) atoms increases to 2.50 Å in accordance with a smaller atomic size of Ni.

Re and Ru substitutions decrease both C_{11} and C_{12}, and as a result, the bulk modulus B=$(C_{11} + 2C_{12})/3$ is significantly reduced. However, the tetragonal shear modulus G'=$(C_{11} - C_{12})/2$ increases slightly with these impurities. Comparison of changes in volume (increases of 10% and 9% for Re and Ru, respectively) and in bulk modulus B (decreases of 13% and 18% for Re and Ru, respectively) shows that not only lattice expansion is responsible for the reduction of B. As can be seen from the calculated charge density maps, ruthenium leads to a weakening of chemical bonds in the first coordination sphere (Fig. 1). The calculated densities of states (DOS) for fcc Ni, Ni-3at.% Re, Ni-3at.% Ru (Fig. 2) demonstrate the changes in electronic structure are due to impurities. The Fermi level E_F in fcc Ni is located on the slope almost of the completely filled Ni3*d* band. The large density of states at the Fermi level N(E_F) favors a metallic conductivity and a high specific heat in fcc Ni. For Ni-3at.% Re, the Fermi level E_F falls into a pseudogap between the filled bonding and empty antibonding 5*d*-states of rhenium. The contribution of Re5*d* states near E_F is small and rhenium impurity leads to a decrease in N(E_F), (Table 1, Figure 2).

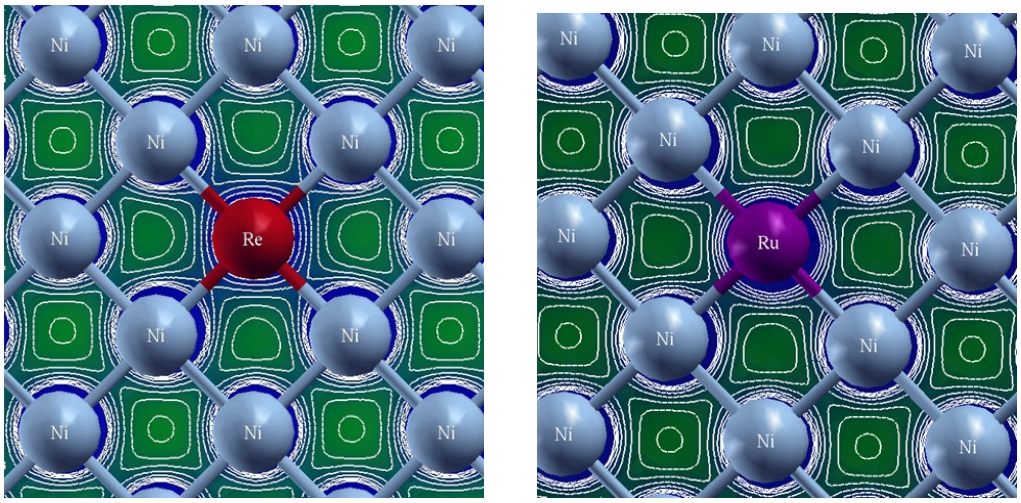

(a) (b)

FIG. 1. Charge density plot for Ni-3at.%Re (a) and Ni-3at.%Ru (b)

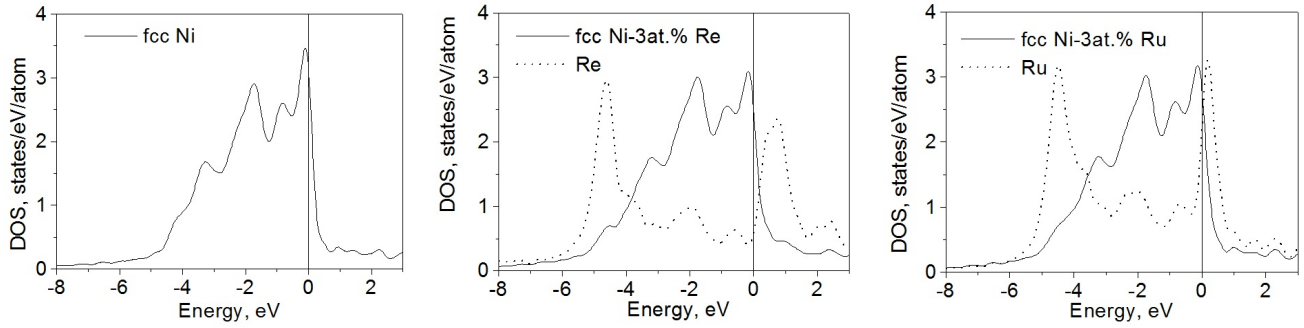

(a) (b) (c)

FIG. 2. Density of d-states for fcc Ni (a), Ni-3at.%Re (b) and Ni-3at.%Ru (c)

TABLE 1. Lattice parameters and elastic parameters for fcc Ni and Ni-3%(Re,Ru)

	Ni	Ni-3at.%Re	Ni-3at.%Ru
a, Å	3.518 3.520 [14] 3.540 [25]	3.5299	3.5286
C_{11}, GPa	239 248 [14] 323 [25]	218	213
C_{12}, GPa	152 155 [14] 162 [25]	126	117
C_{44}, GPa	127 124 [14] 39 [25]	131	126
B, GPa	181 186 [14] 207 [25]	157	149
G, GPa	44 54 [14] 83 [25]	46	48

For Ni-3at.% Ru, the increase in the number of valence electrons due to ruthenium leads to a shift of E_F to a high peak of Ru4d antibonding states (Fig. 2). Contributions from Ru4d and Ni3d states are equal near E_F, and the value of $N(E_F)$ changes little with Ru concentration. It should be noted that the Fermi level is within the range of abrupt changes in DOS (sharp increase in the density of Ru4d states), which may indicate the presence of anelectronic topological transition near 3at.% Ru.

To compare the solubility of these impurities, we calculated the mixing energies E_{mix} as a difference between total energy of alloy and its constituent elements. We obtained E_{mix} to be -0.016 eV and +0.005 eV for 3at.% concentration of Re and Ru additions, respectively. Thus, the solubility of rhenium in fcc Ni should be higher than that of ruthenium.

3.2. Stability of 15 phases in Ni-Re-Ru, Cr-Re-Ru, Mo-Re-Ru and W-Re-Ru systems

First, we optimized the lattice parameters (Table 2) and found the small differences in volumes of the A15 and ground state (fcc, bcc, hcp, hcp, bcc, bcc, respectively) phases of Ni, Cr, Re, Ru, Mo and W. For example, the calculated lattice constant of A15 Cr is equal to 4.545 Å (experiment provides 4.576 Å [26]) and the volume of A15 Cr is 11.736 Å^3/atom that is close to volume of 11.661 Å^3/atom for antiferromagnetic bcc Cr. Lattice parameter of A15 M_3X, where the metal atoms with coordinates (0, 0, 0) are replaced by X = Re or Ru, increases in accordance with the larger atomic size of the X atom. Ruthenium and rhenium increase the lattice parameter of the A15 phase based on 3d metals by 2% and almost do no influence on the lattice parameter is exerted by molybdenum-and tungsten-containing A15

phases. Comparison with fcc Ni shows that a lattice misfit between fcc Ni and A15 Cr is small (2.4%) and increases up to 14% for the A15 W and A15 Mo.

TABLE 2. Lattice parameter a, density of states at the Fermi level $N(E_F)$ and enthalpy formation ΔH for A15 phases in Ni–Re–Ru, Cr–Re–Ru, Mo–Re–Ru and W–Re–Ru systems

Phase	a, Å	$N(E_F)$, state/eV	ΔH (eV/atom)	Phase	a, Å	$N(E_F)$ state/eV	ΔH (eV/atom)
Ni	4.461	3.81	+0.084	Cr_3Re	4.648	1.27	+0.048
Cr	4.545	0.61	+0.071	Cr_3Ru	4.613	2.15	+0.080
Re	4.945	1.41	+0.160	$Cr_3Re_{0.5}Ru_{0.5}$	4.633	1.32	+0.060
Ru	4.923	0.94	+0.422	Mo_3Re	4.993	1.02	+0.005
Mo	5.023	0.54	+0.090	Mo_3Ru	4.964	1.21	+0.027
W	5.057	0.51	+0.122	$Mo_3Re_{0.5}Ru_{0.5}$	4.979	1.19	+0.018
Ni_3Re	4.574	1.62	+0.106	W_3Re	5.017	3.24	+0.034
Ni_3Ru	4.572	3.24	+0.204	W_3Ru	4.988	1.03	+0.091
$Ni_3Re_{0.5}Ru_{0.5}$	4.633	1.32	+0.127	$W_3Re_{0.5}Ru_{0.5}$	5.004	1.87	+0.064

The enthalpy of formation, ΔH, calculated relative to the total energies of elemental metals is positive for all A15 phases (Table 2). As one can see (Table 2), group VI metals (Cr,Mo) and Ni form A15 phases with enthalpies of formation less than 0.1 eV/atom. For elemental A15 phases, stability increases in the series: Cr > Ni > Mo > W > Re > Ru and the most stable A15 phases correspond to Cr, Ni and Mo, while A15 Ru is the most unstable. For binary A15 phases, stability increases as Mo_3Re > W_3Re > Cr_3Re > Ni_3Re and Mo_3Ru > Cr_3Ru > W_3Ru > Ni_3Ru (Table 2). Among the A15 M_3Re phases, very small positive values of ΔH were obtained for Cr_3Re (+0.048 eV/atom), Mo_3Re (+0.005 eV/atom) and W_3Re (+0.034 eV/atom), which are lower than those for the unalloyed A15 phases without Re. Thus, we conclude that formation of the metastable A15 phases should be more favorable in binary alloys with Re addition. However, ΔH is higher for Ni_3Re than for A15 Ni and the addition of Re in Ni matrix should not lead to the appearance of Ni-Re particles. The simultaneous presence of Re and the group VI metals in a Ni matrix favors the formation of close-packed A15 particles, which explains the experimental finding on the effect of Cr, Mo and W additions on the appearance of TCP phases.

The formation enthalpy of A15 phases with ruthenium is higher by 2-3 times than with rhenium and A15 M_3Ru is less stable for all considered metals M. There is a correlation between stability and density of states at the Fermi level, where the value $N(E_F)$ is less for the more stable phase. As shown in Fig. 3, the Fermi level E_F lies within the antibonding states for both Cr_3Re and Cr_3Ru. The larger number of valence Ru d-electrons in Cr_3Ru results in a shift of the Fermi level at a peak of antibonding states that weaken the bonding compared to Cr_3Re (Fig. 3). The ternary $Mo_3Re_{0.5}Ru_{0.5}$ and $W_3Re_{0.5}Ru_{0.5}$ are even more stable than the corresponding A15 metal phases, however, ruthenium destabilizes the all A15 M_3Re phases and ΔH increases as $Mo_3Re_{0.5}Ru_{0.5}$ >$Cr_3Re_{0.5}Ru_{0.5}$ >$W_3Re_{0.5}Ru_{0.5}$ > $Ni_3Re_{0.5}Ru_{0.5}$.

To predict the elastic properties and mechanical stability of A15 phase, we calculated the elastic parameters for Mo_3Re, $Mo_3Re_{0.5}Ru_{0.5}$ and Mo_3Ru which are the most stable

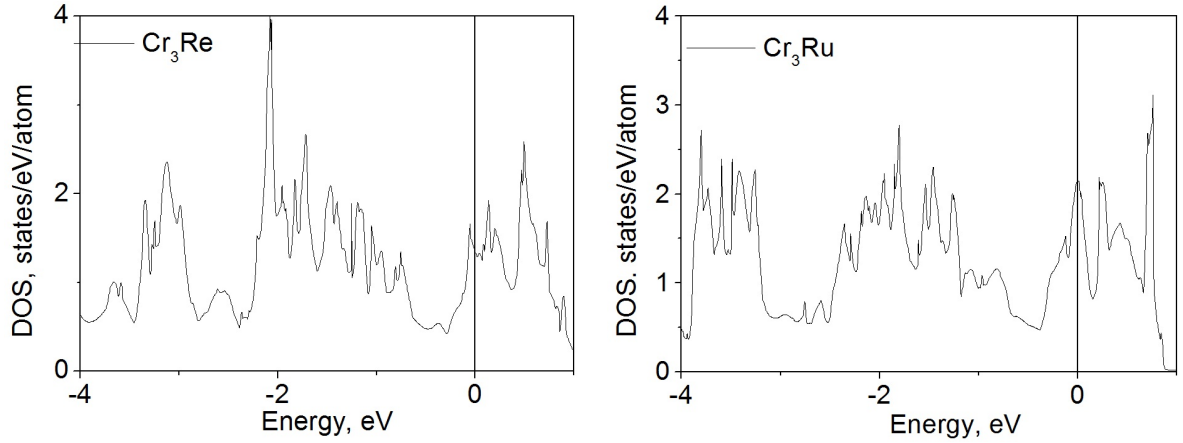

(a) (b)

FIG. 3. Density of d-states for 15 Cr_3Re (a) and Cr_3Ru (b). The Fermi level is at zero

among the considered A15 phases (Table 3). We found that ruthenium reduces the elastic constants C_{11}, C_{12} and C_{44} in accord with the weaker bonding in the Ru systems. The mechanical stability of cubic crystal requires $C_{11}-C_{12}>0$, $C_{11}>0$, $C_{44}>0$, $C_{11}-2C_{12}>0$. As shown in Table 3, the elastic constants obey these stability criteria for all A15 Mo–Re and Mo–Ru phases.

TABLE 3. Elastic constants and moduli, anisotropy A and G/B for Mo_3Re, $Mo_3Re_{0.5}Ru_{0.5}$, Mo_3Ru

	C_{11}	C_{12}	C_{44}	B	G	A	G/B
Mo_3Re	499	190	98	293	154	0.64	0.52
$Mo_3Re_{0.5}Ru_{0.5}$	486	176	94	279	155	0.61	0.55
Mo_3Ru	465	175	87	272	145	0.60	0.53

Bulk and tetragonal shear moduli were calculated as $B=(C_{11}+2C_{12})/3$ and $G=(C_{11}-C_{12})/2$. It is seen (Table 3) that both bulk modulus B and shear modulus G decrease with ruthenium. The anisotropy factor, calculated as $A=2C_{44}/(C_{11}-C_{12})$, shows that all phases are anisotropic ($A\neq 1$), and the presence of ruthenium does not affect the anisotropy of elastic deformations. The ratio of G/B represents the Pugh's criterion [27]: a material behaves in a ductile manner if $G/B<0.57$ and demonstrates brittleness when $G/B>0.57$. For all the considered A15 phases, G/B is close to 0.57 and these phases should not have a plastic behavior, but rather demonstrate a tendency to be brittle and fracture.

4. Conclusions

Ab-initio calculations were performed to elucidate the effect of rhenium and ruthenium on the electronic structure and elastic properties of fcc Ni as well as on the stability of TCP phases. Both rhenium and ruthenium additions increase the lattice parameter and reduce the bulk modulus of fcc Ni, whereas the tetragonal shear only varies slightly. We found that the solubility of rhenium in fcc Ni should be higher than that of ruthenium. We established that the presence of chromium, molybdenum and tungsten favors to the formation of closely packed particles in rhenium containing nickel matrix and the concentration of

these additions should be restricted in an alloy. The TCP particles are mechanically stable and their formation enthalpy is close to zero. Molybdenum has the greatest tendency to form TCP phases with A15 structure. The mechanism by which ruthenium exerts a positive effect on TCP particle formation is related to its decrease of their stability.

Acknowledgments

This work was supported by Research Program of Ural Branch of the RAS, Grant No. 12-U-3-1007.

References

[1] Darolia R., Lahrman D.F., Field R.D., *Superalloys* 1988 Edited by S. Reichman, D.N. Duhl, G. Maurer, S. Antolovich and C. Lund. The Metallurgical Society, p. 255 (1988).
[2] Bhadeshia H. K. D. H. *Nickel Based Superalloys*. University of Cambridge. http://www.msm.cam.ac.uk/phase-trans/2003/Superalloys/superalloys.html
[3] Reed R.C. *The Superalloys: Fundamentals and Applications*. Cambridge University Press, Cambridge (2006).
[4] Argence D., Vernault C, Desvallees Y, Fournier D. II Superalloys 2000. Eds. T.M. Pollock, R.D. Kissinger, R.R. Bowman et al. Champion (Pennsylvania). P. 829 (2000).
[5] Kablov E.N., Petrushin N.V. Physicochemical and technological features of creating metal-based high-superalloys. *Pure Appl. Chem.*, **076**(9), P. 1679–1689 (2004).
[6] Sims S. T. In Superalloys II, S. T. Sims, N. S. Stoloff, W. C. *Hagel* (Eds.), P. 217–240, Wiley-Interscience, New York (1987).
[7] Caron P. High γ' Solvus New Generation Nickel-based Superalloys for Single Crystal Turbine Blade Applications. Superalloys 2000, ed. T.M. Pollock, et al, (Warrendale, PA: TMS, 1996), P. 737–746.
[8] Murakami H., Honma T., Koizumi Y., Harada H., in:T.M. Pollock, R.D. Kissinger, R.R. Bowman, K.A. Green, M. McLean, S.L. Olson, J.J. Schirra (Eds.), Superalloys 2000, TMS, Champion, PA, 2000, p. 747.
[9] Koizumi Y, Kobayashi T., and Yokokawa T. at al. Development of next-generation of Ni-base single crystal superalloys. II Superalloys 2004 / Eds. by K.A. Green et al. Champion (Pennsylvania), 2004. P. 35–43.
[10] O'Hara K.S., Walston W.S., Ross , Darolia R. US Patent No 5482789.09.01.1996.
[11] Sato A., Harada H., Yokokawa T., Murakumo T., Koizumi Y., Kobayashi T., Imai H. The effects of ruthenium on the phase stability of fourth generation Ni-base single crystal superalloys. *Scripta Mater*, **54**(9), P. 1679–1684 (2006).
[12] L.J. Carroll, Q. Feng, J.F. Mansfield, T.M. Pollock, High Refractory, Low Misfit Ru-Containing Single-Crystal Superalloys. *Met. Mat. Trans.*, **37A**, P. 2927–2938 (2006).
[13] Tournier S, Vinet B, Pasturel A, Ansara I, Desre' PJ. Undercooling-induced metastable A15 phase in the Re-W system from drop-tube processing. *Phys Rev B*, **57**(6), P. 3340–3344 (1998).
[14] Federer JI, Steele RM. Identification of a Beta-Tungsten Phase in Tungsten-Rhenium Alloys. *Nature*, London, **205**, P. 587–588 (1965).
[15] Chu JP, Chang JW, Lee PY. Phase Transformation of A15 crystal structure chromium thin films grown by the sputter-deposition. *Mater Chem Phys.*, **50**(1), P. 31–36 (1997).
[16] Chu JP, Chang JW, Lee PY, Wu JK, Wang JY. On the formation of nonequlibrium A15 crystal structure chromium thin films grown by the sputter-deposition. *Thin Solid Films.* **312**(1-2), P. 78–85 (1998).
[17] Turchi PEA, Finel A. Ordering phenomena in *A*15-based alloys. *Phys Rev B*, **46**, P. 702–725 (1992).
[18] Medvedeva N.I., Gornostyrev Y.N., Freeman A.J., Carbon stabilized A15 Cr_3Re precipitates and ductility enhancement of Cr-based alloys. *Acta Mater.*, **50**(10), P. 2471–2476 (2002).
[19] Medvedeva N.I., Gornostyrev Y.N., Freeman A.J., Structural properties, electronic structure, Fermi surface, and mechanical behavior of bcc Cr-Re alloys. *Phys. Rev. B*, **67**(13), P. 134204-6 (2003).
[20] Hummershschmidt T., Seiser B., Pettifor, Superalloys-2012, Edited by E.S.Huron, et al, Willey TMS, p. 138
[21] Kresse G., Joubert D. From ultrasoft pseudopotentials to the projector augmented-wave method. *Phys. Rev. B*, **59**(3), P. 1758–756 (1999).

[22] Kresse G., Furthmüller J. Efficient iterative schemes for ab initio total-energy calculations using a plane-wave basis set. *Phys. Rev. B.*, **54**(16), P. 11169–11186 (1996).
[23] Perdew, K. Burke, M. Ernzerhof, Generalized gradient approximation made simple. *Phys. Rev. Lett.*, **77**(18), P. 3865–3868 (1996).
[24] Gorbunov J.P., Levin A.A., Mensch A., Meyer D.C., Tselev A., Paufler P., Pompe W., Eckert D. Formation of unusual intermetallic phases by vacuum PLD. *Applied Surface Sci.*, **B197**(3), P. 475–480 (2002).
[25] Guo G.Y., Wang H.H. Gradient-Corrected Density Functional Calculation of Elastic Constants of Fe, Co and Ni in bcc, fcc and hcp Structures. *Chinese J. Phys.*, **38**(5), P. 949–961 (2000).
[26] Kimoto K., Nishida I. An electron diffraction study on the crystal structure of a new modification of chromium. *J. Phys. Soc. Japan*, **22**(3), P. 744–756 (1967).
[27] Pugh S. F. Relations between the elastic moduli and the plastic properties of polycrystalline pure metals. *Phil. Mag.*, **45**(367), P. 823–843 (1953).